

# F<sub>2</sub>-Laser Microfabrication of Diffractive Phase Elements

M. Pfeifer, F. Jahn, A. Kratsch, B. Steiger and S. Weissmantel

*University of Applied Sciences Mittweida, Technikumplatz 17, 09648 Mittweida, Germany*

**Keywords:** DPE, Diffractive Phase Element, DOE, Diffractive Optical Element, Fluorine Laser, Mask Projection.

**Abstract:** Fluorine laser microfabrication enables direct structuring of diffractive phase elements in fused silica. These elements are used as beam shapers for the wide wavelength range from 248 to 1100 nm. We present selected phase elements for laser beam shaping in the visible wavelength range. Furthermore we show the laser beam shaping of a fiber laser with a wavelength of  $\lambda = 1070$  nm. The main advantage of this application is the much more compact design compared with the current used method of beam shaping by conventional optics. Fluorine laser microstructuring provides an effective alternative to lithography techniques. It is a fast and individual method to fabricate customized or prototype diffractive phase elements in a cost-effective way.

## 1 INTRODUCTION

Beam shaping by diffractive phase elements (DPEs) is currently one of the most important fields of research on optics with almost the greatest potential in application and innovation. In the future it will be possible to shape any beam profile into almost every desired beam distribution. In this way DPEs enable the homogenization of laser beams. The main advantage of this application is the much more compact design compared with the current used method of beam homogenization by conventional optics. Furthermore, it is conceivable to design special DPEs shaping the raw laser beam directly into the desired beam geometry for the working plane. In this way, masks are no longer needed. Thus the laser power can be used more efficiently by using the full beam cross-section.

The manufacturing of DPEs is mainly done by photolithography. This technique is very complex, because it has to be done in several photolithography steps. Also it requires a various number of masks due to the desired number of steps of the DPE. Laser microstructuring using a mask projection technique opens up a new way. It is a fast and individual technique to fabricate customized or prototype diffractive phase elements in a cost-effective way. This is possible because, for instance, compared with photolithography there are no special masks necessary, which have to be manufactured for each new DPE. Also there is only one mask needed,

because of the pixelwise structuring process. The microstructuring is done by pulsed laser ablation using a fluorine laser. Because of its short wavelength in the VUV range, it enables micromachining of wide band gap materials such as fused silica. Furthermore, calcium fluoride is used as material for beam shapers for the excimer laser wavelength 157 nm and 193 nm. However, this material is very difficult to structure by lithography techniques because of its material properties. Fluorine laser microstructuring provides an effective alternative at this point.

## 2 F<sub>2</sub>-LASER STATION

The microstructuring is done by a fully automated high-precision laser micromachining station. It was developed and built by 3D-Micromac AG in cooperation with the University of Applied Sciences Mittweida. A fluorine laser LPF 220i of Coherent (Deutschland) GmbH is integrated in this station. The laser beam has a wavelength of 157 nm that corresponds to a photon energy of 7.9 eV. The maximum repetition rate is 200 Hz and the pulse duration is 25 ns. The pulse energy can be varied from 10 to 30 mJ. Because of the wavelength in the VUV range, the beam guidance must take place in an oxygen-free atmosphere. The special advantage of the used laser station is a system of two independent vacuum chambers. After evacuation

these chambers are flooded with pure nitrogen (5.0) to normal pressure.

The laser microstructuring is done by mask projection technique. Here the mask geometry is optically imaged onto the substrate surface by a transmission objective with a demagnification ratio of 26 : 1. The maximum structure size on the substrate surface is about  $225 \times 225 \mu\text{m}^2$  with a resolution of  $< 1 \mu\text{m}$ . The maximum possible laser pulse fluence on the substrate surface is about  $7 \text{ J/cm}^2$ .

### 3 DESIGN OF DIFFRACTIVE PHASE ELEMENTS

Diffraction phase elements are a special kind of diffractive optical elements. The active principle is the modulation of the phasing of the electromagnetic wave. The phase displacement between the points on the wave front is provided by different optical path lengths, which is achieved by structuring of different step heights. This leads to the intended diffraction effects and therefore to the generation of defined diffraction images. Fused silica is used as substrate material because of its good transmission properties over a wide spectral range.

The calculation of the DPEs is based on a variant of the well known POCS-method (projection onto convex sets) (Ersoy, 2007). Here the given field strength distributions are addressed as boundary conditions at the DPE and pictorial space. Both, the input-sided intensity distribution and the distribution in the target plane, i.e. the desired diffraction image, must be given. The transition between the spaces is mathematically done by propagation operators. The most frequently used operator is the Fourier transformation and the inverse Fourier transformation, respectively. Therefore, this procedure is state of the art in various versions as so-called iterative Fourier transform algorithm (IFTA) (Fienup, 1982; Ripoll, Kettunen and Herzig, 2004; Kim, Yang and Lee, 2004). The convergence of this algorithm thereby depends on various parameters. A good result for the phase distribution of the intended DPE is reached after approximately 30 iteration steps.

A detail of such a phase distribution is shown in Figure 1. Here a defined phasing is assigned to each gray value. The phase distribution of the DPE is completely irregularly based on the unsymmetrical intensity distribution in the target plane.

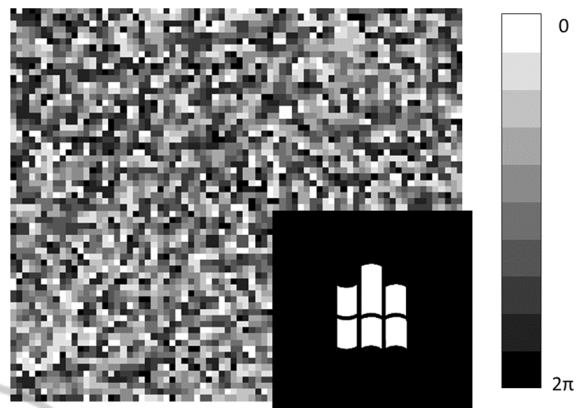


Figure 1: Detail of the phase distribution and target structure of a nine level DPE producing the logo of the University of Applied Sciences Mittweida (array of  $128 \times 128$  pixels).

The original quasi-continuously calculated distribution is discretized during the algorithm both in its allocation and regarding to the possible phasing. This creates the shown pixel-like structure. This discretization is due to the properties of the manufacturing technology. The higher diffraction orders indicated in Figure 2 are a disadvantage of this simplification. This leads to a loss of power in laser beam shaping.

The applying of the Fourier transformation as propagation operator between DPE and pictorial space creates so-called Fourier elements. Their diffraction image is basically formed in the far field in infinite distance. However, a distance which is very large towards the pixel size becomes practically sufficient. In the academic literature different criteria are defined for the quantitative determination of the minimum distance (Lipson, Lipson and Tannhauser, 1997; Träger, 2007). Such DPEs are used for alignment applications because of their almost constant image quality over long distances.

With special regard to the practical application of laser beam shaping for laser material processing often there is defined a clear target plane, in which the desired image should be formed sharply. This is done by additional phase terms, which allow a further manipulation of the diffraction image. For instance, a spherical lens term enables the sharply image formation in a defined target plane.

Figure 2 shows the simulated diffraction image of a DPE producing the logo of the University of Applied Sciences Mittweida in different projection distances. The phase distribution of this DPE contains a spherical lens term with a focal length of 300 mm. As a result the diffraction image is formed

sharply only in the focus. The absolute size of the created structure depends on the projection distance.

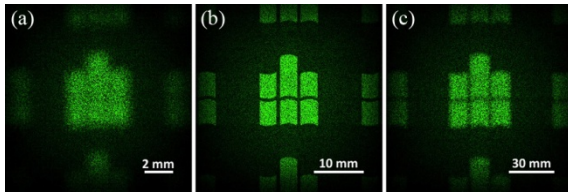


Figure 2: Simulated diffraction image of a nine level DPE producing the logo of the University of Applied Sciences Mittweida (array of  $256 \times 256$  pixels, pixel size:  $7.8 \times 7.8 \mu\text{m}^2$ , design wavelength:  $532 \text{ nm}$ ) with a spherical lens term with a focal length of  $300 \text{ mm}$  in a projection distance of (a)  $0.1 \text{ m}$ , (b)  $0.3 \text{ m}$ , and (c)  $1 \text{ m}$ .

The simulation of the shown diffraction images is done by numerical simulation software based on the real expected DPE structures. Therefore besides VirtualLab<sup>TM</sup> 5.3 of LightTrans GmbH also self-created program scripts for MATLAB<sup>®</sup> of MathWorks are used. Here the advantage is, besides the possibility of control, that the influence of different parameters on the formed diffraction image of the DPE can be examined. In this way the cost-intensive manufacturing of many different DPEs by the trial-and-error method is no longer necessary.

Beside the elementary parameters pixel size, number of pixels, and number of steps, a major impact on the final diffraction image is particularly caused by manufacturing-related deviations from the ideal calculated phase distribution. Fluctuations of the laser fluence during the structuring process result in deviations in the structure depth. Form deviations of the pixels are due to defects in the imaging system. Based on these deviations the quality of the diffraction image declines, which is shown by Olbrich, Fischer and Steiger (2012). An essential characteristic of that is the formation of an intensive peak in the middle of the diffraction orders.

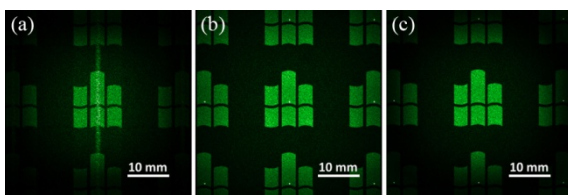


Figure 3: Simulated diffraction image of a DPE having regard to real manufacturing faults: (a) fluctuations of the laser fluence, (b) bars between the pixels, and (c) rounded pixel corners.

Figure 3 shows the influences of the deviations on the known diffraction image of the university logo. Not only incorrect structure depth (see

Figure 3(a)), but also bars between the pixels (see Figure 3(b)) and rounded corners of the normally quadratic pixels (see Figure 3(c)) alter the diffraction image. In these figures the formation of the centered peak is clearly visible in each diffraction order. Furthermore, Olbrich, Fischer and Steiger (2012) show that surface roughness and process-related debris on the DPE surface lead to an increased background noise in the surrounding of the zeroth diffraction order. Practically a mixture of the shown phenomena can be expected according to the influence of each error at the manufacturing process.

Such an intensity peak is absolutely counterproductive for beam shaping for laser material processing. Thus strategies have to be developed to completely prevent these peaks or at least to reduce their negative effects. A possible approach could be the method of  $\text{CO}_2$  laser smoothing mentioned below. Another possibility consists in the use of the already mentioned additional phase terms. The separation of the target structure from the centered peak is possible by using a linear wedge term, which causes a shift of the target structure by a defined angle.

The theoretical phase modulations must be transferred into an appropriate form to manufacture the designed DPEs by fluorine laser microstructuring. Therefore, the determined phase information is transferred to be structured depth for each pixel according to the design wavelength and the refractive index of the substrate. The fluorine laser microstructuring of the DPEs is done with masks out of tantalum foil with quadratic aperture. Here the mask size is selected according to its image size in the working plane, which corresponds to the desired pixel size.

## 4 RESULTS AND DISCUSSION

### 4.1 DPEs with a Lens Term for $\Lambda = 532 \text{ Nm}$

The DPEs are structured in Corning 7980 (fused silica). They have nine levels with a structure height of  $120 \text{ nm}$  per step, designed for a wavelength of  $\lambda = 532 \text{ nm}$ . Figure 4 shows an optical micrograph of a DPE producing the logo of the University of Applied Sciences Mittweida.

Figure 5 shows the diffraction image of this DPE in a projection distance of  $1.68 \text{ m}$ .

The target structure is clearly visible, but the diffraction orders are overlaid by a centered peak.

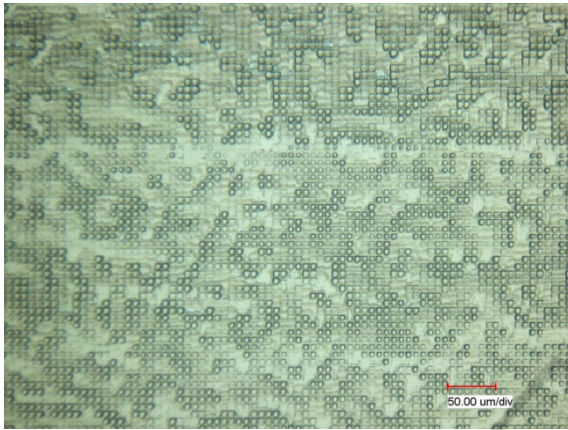


Figure 4: Optical micrograph of a nine level DPE producing the logo of the University of Applied Sciences Mittweida (array of  $256 \times 256$  pixels, pixel size:  $7.8 \times 7.8 \mu\text{m}^2$ , design wavelength: 532 nm).

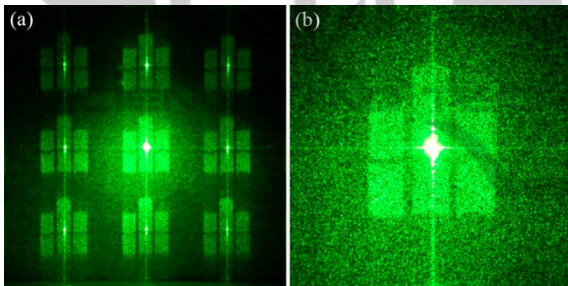


Figure 5: Diffraction image of the DPE shown in Figure 4 in a projection distance of 1.68 m.

The main cause is an overlaid diffraction grating based on undesirable bars between the pixels. Basically, their formation can be averted. The formation of the higher diffraction orders is due to the discretization of the DPEs in the pixel-like structure, as mentioned before. This was already shown in the simulation. The formation of these diffraction orders can only be avoided by a continuous transition of the height profile.

The DPE shown in Figure 4 is calculated with an image formation in the infinite. The function of a DPE with lens term is shown in Figure 6. This DPE differs to the previous by an additional spherical lens term with a focal length of 300 mm (cf. Figure 2). The diffraction image is shown in different projection distances.

The real diffraction images are similar to the simulated ones. It becomes clear, that just like in the simulation the diffraction image becomes blurred faster towards a shorter projection distance than towards a longer one.

A comparison of the diffraction images in Figure 5(b) and Figure 6(b) shows, that the

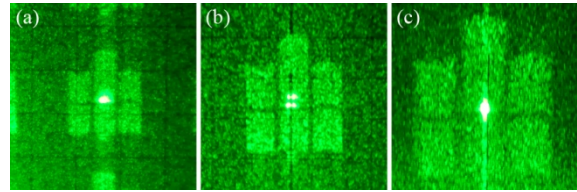


Figure 6: Diffraction image of the DPE described in Figure 2 in a projection distance of (a) 0.2 m, (b) 0.3 m, and (c) 1 m.

diffraction image of the DPE with lens term is more detailed and has sharper contours than the DPE without a lens term. Thus the partially blur of the diffraction image of the DPE without a lens term is not caused by a worse structuring. The diffraction image should be captured in a longer projection distance.

#### 4.2 DPE with a Wedge Term for $\Lambda = 633 \text{ Nm}$

To separate the target structure from the centered peak, a DPE with a linear wedge term was structured. It is an eleven level DPE with a structure height of 120 nm per step, designed for a wavelength of  $\lambda = 633 \text{ nm}$ . The target structure of this DPE is the same as before. It is also designed with an additional spherical lens term, but with a focal length of 320 mm.

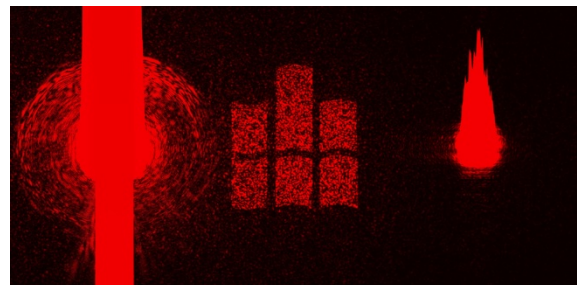


Figure 7: Diffraction image of an eleven level DPE producing the logo of the University of Applied Sciences Mittweida (array of  $256 \times 256$  pixels, pixel size:  $10 \times 10 \mu\text{m}^2$ , design wavelength: 633 nm) with a spherical lens term with a focal length of 320 mm and a linear wedge term captured in focus.

The diffraction image of the DPE is shown in Figure 7. The target structure is shifted by a defined angle and therefore it is completely separated from the centered peak. The red stripe on the left side of the image is not a part of the diffraction image. It is a saturation effect of the CCD sensor. Also the circular halo effect is a result of undesired reflections at the beam expander.

### 4.3 Beam Shaper for a Fiber Laser with $\lambda = 1070 \text{ Nm}$

Based on the investigations above a DPE was manufactured to shape a fiber laser beam with a wavelength of  $\lambda = 1070 \text{ nm}$  into the known target structure. The DPE has 19 levels with a structure height of 120 nm per step. The DPE is designed with an additional spherical lens term with a focal length of 100 mm and a linear wedge term.

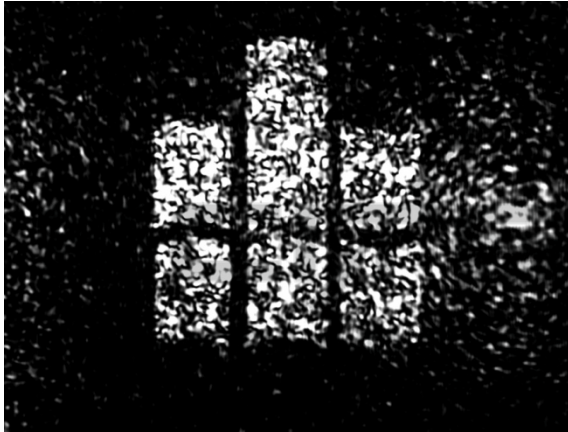


Figure 8: Diffraction image of a 19 level DPE producing the logo of the University of Applied Sciences Mittweida (array of  $160 \times 160$  pixels, pixel size:  $22.3 \times 22.3 \mu\text{m}^2$ , design wavelength: 1070 nm) with a spherical lens term with a focal length of 100 mm and a linear wedge term captured in focus.

The diffraction image of the DPE is shown in Figure 8. The centered peaks are not very pronounced due to a reducing of the undesirable bars between the pixels. There is only some background noise in the surrounding of the zeroth diffraction order, as mentioned before. Thus the laser beam shaping for an ytterbium-doped fiber laser was successfully done.

Besides a DPE for laser beam shaping of a diode laser with a wavelength of  $\lambda = 940 \text{ nm}$  was manufactured. It was already tested at a laser power up to 1 kW in cw mode for a short time without any damage of the DPE.

### 4.4 CO<sub>2</sub> Laser Smoothing of DPEs

Bars could occur between the pixels, as mentioned in chapter 4.1. These undesirable bars have a negative impact on the diffraction image so far as they produce a diffraction image of the raw laser beam. This second diffraction image overlays the desired ones (cf. Figure 5(a)). Another problem is a

roughening of the surface caused by the laser microstructuring process. This leads to a blur of the diffraction image. Both the reducing of the surface roughness and the removal of the undesirable bars is done by temperature controlled CO<sub>2</sub> laser smoothing.

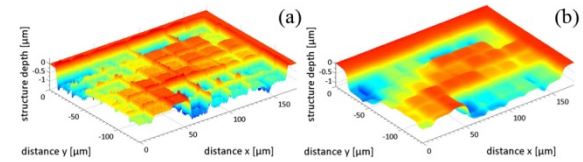


Figure 9: Three-dimensional confocal micrograph of a DPE producing an "F" (array of  $50 \times 50$  pixels, pixel size:  $21 \times 21 \mu\text{m}^2$ , design wavelength: 532 nm) (a) before and (b) after CO<sub>2</sub> laser smoothing.

Figure 9 shows the confocal micrograph of the DPE before and after CO<sub>2</sub> laser smoothing. The related profiles are shown in Figure 10.

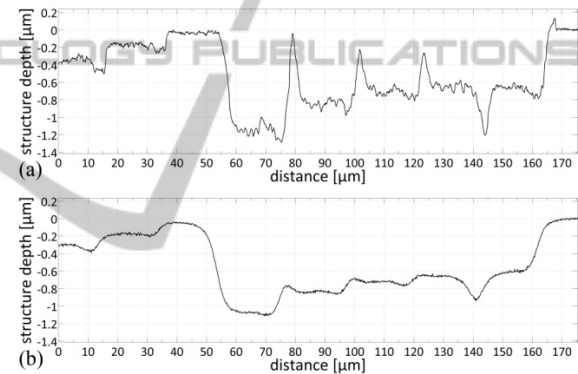


Figure 10: Profile of selected pixels of the DPE shown in Figure 9 (a) before and (b) after CO<sub>2</sub> laser smoothing.

The success of the technique is clearly visible. The undesirable bars between the pixels are almost completely removed. The quadratic surface roughness could be improved from  $S_q = 44.9 \text{ nm}$  to  $S_q = 20.3 \text{ nm}$ . These are averaged values over 25 pixels with different structure depths. The roughness depends on the structure depth. The roughness of the unstructured surface is  $S_q = 8.9 \text{ nm}$ .

The diffraction image of the DPE before and after CO<sub>2</sub> laser smoothing is shown in Figure 11.

A comparison of Figure 11(a) and Figure 11(c) shows, that the centered peaks are only weakly visible due to the removing of the undesirable bars between the pixels. Also the higher diffraction orders are less pronounced after smoothing, which comes along with an increase of the laser beam intensity in the zeroth diffraction order. As this diffraction order is more pronounced and has sharper

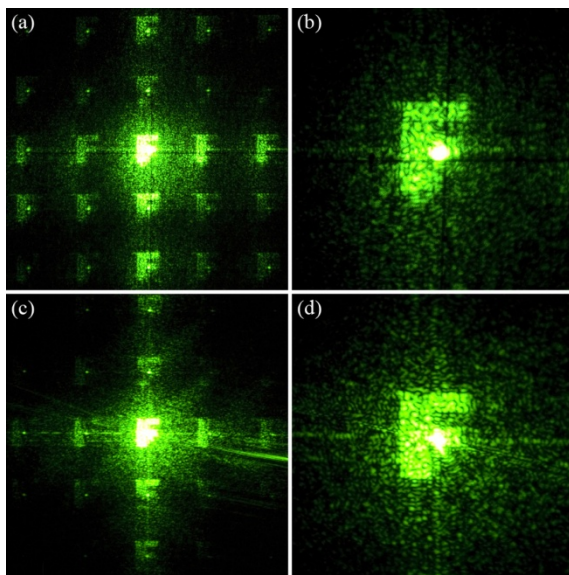


Figure 11: Diffraction image of the DPE shown in Figure 9 in a projection distance of 1 m (a), (b) before and (c), (d) after CO<sub>2</sub> laser smoothing.

contours, which can be seen in Figure 11(d) compared with Figure 11(b). This effect is due to a redistribution of the glass by the CO<sub>2</sub> laser smoothing. Thus the edges of the pixels are rounded and the pixel-like structure becomes more a kind of continuous transition of the height profile.

## 5 CONCLUSIONS

The microstructuring of diffractive phase elements by fluorine laser is possible. Both the function of DPEs with image formation in the infinite and in a defined projection distance could be shown. Furthermore, the function of an additional wedge term was shown, which separate the target structure from the centered peak. On basis of these investigations a DPE was manufactured to shape a fiber laser beam, which could successfully be shown.

The image quality of the diffraction images of the DPEs could be improved by CO<sub>2</sub> laser smoothing. The undesirable bars were almost completely removed and the surface roughness smoothed.

## ACKNOWLEDGEMENTS

The authors gratefully acknowledge financial support of the present work by the Federal Ministry

of Education and Research (FKZ: 16V0053), the European Union and the Free State of Saxony.

## REFERENCES

- Ersoy, O., 2007. *Diffraction, Fourier Optics and Imaging*, Wiley. Hoboken, 1<sup>st</sup> edition.
- Fienup, J. R., 1982. Phase retrieval algorithms: a comparison. In *Applied Optics*, 21(15), pp.2758-2769.
- Kim, H., Yang, B. and Lee, B., 2004. Iterative Fourier transform algorithm with regularization for the optimal design of diffractive optical elements. In *Journal of the Optical Society of America A* 21(12), pp.2353-2365.
- Lipson, S., Lipson, H. and Tannhauser, D., 1997. *Optik*, Springer. Berlin, 1<sup>st</sup> edition.
- Olbrich, M., Fischer, A. and Steiger, B., 2012. Numerische Simulationen an realen DOE-Strukturen, In *Journal of the University of Applied Sciences Mittweida*, (2), pp.107-111.
- Ripoll, O., Kettunen, V. and Herzig, H.P., 2004. Review of iterative Fourier-transform algorithms for beam shaping applications. In *Optical Engineering*, 43(11), pp.2549-2556.
- Träger, F. ed., 2007. *Springer Handbook of Laser and Optics*, Springer. New York, 1<sup>st</sup> edition.